BIOLOGY LETTERS

royalsocietypublishing.org/journal/rsbl

Research

Cite this article: Pérez-Ramos A, Romero A, Rodriguez E, Figueirido B. 2020 Three-dimensional dental topography and feeding ecology in the extinct cave bear. *Biol. Lett.* **16**: 20200792.
https://doi.org/10.1098/rsbl.2020.0792

Received: 3 November 2020
Accepted: 1 December 2020

Subject Areas:
palaeontology, evolution, ecology

Keywords:
cave bears, dental topography, feeding behaviour, evolution

Author for correspondence:
Borja Figueirido
e-mail: borja.figueirido@uma.es

Electronic supplementary material is available online at https://doi.org/10.6084/m9.figshare.c.5237654.

THE ROYAL SOCIETY PUBLISHING

Palaeontology

Three-dimensional dental topography and feeding ecology in the extinct cave bear

Alejandro Pérez-Ramos[1], Alejandro Romero[2], Ernesto Rodriguez[1] and Borja Figueirido[1]

[1]Departamento de Ecología y Geología, Facultad de Ciencias, Universidad de Málaga, 29071 Málaga, Spain
[2]Departamento de Biotecnología, Facultad de Ciencias, Universidad de Alicante, 03080 Alicante, Spain

AP-R, 0000-0003-1417-4338; AR, 0000-0002-5743-0613; BF, 0000-0003-2542-3977

The cave bear (*Ursus spelaeus s.l.*) was an iconic extinct bear that inhabited the Pleistocene of Eurasia. The cause of extinction of this species is unclear and to identify the actual factors, it is crucial to understand its feeding preferences. Here, we quantified the shape descriptor metrics in three-dimensional (3D) models of the upper teeth (P^4–M^2) of the cave bear to make inferences about its controversial feeding behaviour. We used comparative samples, including representatives of all living bear species with known diets, as a template. Our topographic analyses show that the complexity of upper tooth rows in living bears is more clearly associated with the mechanical properties of the items consumed than with the type of food. Cave bears exhibit intermediate values on topographic metrics compared with the bamboo-feeder giant panda (*Ailuropoda melanoleuca*) and specialists in hard mast consumption (*Ursus arctos* and *Ursus thibetanus*). The crown topography of cave bear upper teeth suggests that they could chew on tough vegetal resources of low quality with high efficiency, a characteristic that no living bear currently displays. Our results align with a climate-driven hypothesis to explain the extinction of cave bear populations during the Late Pleistocene.

1. Introduction

The cave bear (*Ursus spelaeus s.l.*) is an iconic extinct bear, making up a part of the megafauna that inhabited the Pleistocene of Eurasia, whose extinction causes are controversial. One key aspect of understanding why these cave bears became extinct relates to their feeding behaviour [1]. Some authors propose that cave bears were adapted to feed exclusively on vegetal resources from 100 000 to 20 000 years ago [2], without evidence of a dietary shift towards omnivory at a time of lowered vegetation productivity during the Last Glacial Maximum [3]. Both the lack of dietary flexibility and possible human competition are proposed to be critical factors in explaining the extinction of cave bears [4,5]. Recently, Pérez-Ramos *et al.* [6] demonstrated that large paranasal sinuses were likely selected in cave bears to overcome longer hibernation periods, but the sinuses also compromised the skulls biomechanically. This biomechanical restriction in the skull of cave bears led to a lack of dietary flexibility typical of omnivorous bears. Cave bears exhibited a unique gradual increase in their tooth-root area values of maxillary teeth (P^4–M^2), the values of their most posterior molars approaching those of the bamboo-feeder giant panda (*Ailuropoda melanoleuca*) [7]. Despite this, the topography of maxillary tooth crown surfaces in cave bears has never been studied in detail. Therefore, the motivation of our study was to make inferences on cave bear feeding preferences by investigating the topography of their maxillary teeth [6].

Tooth shape correlates with feeding behaviour because it plays a key role in the mechanical breakdown of food and release of nutrients during chewing [8].

In recent years, the analysis of the three-dimensional (3D) surface of tooth crowns has allowed the quantification of shape descriptors of tooth crown topographies that are associated with masticatory performance and feeding behaviour in mammals [8–10].

Here, we apply a 3D dental topographic analysis to quantify the dental topographic curvature (Dirichlet normal energy, DNE), relief (surface relief index, RFI) and complexity (using orientation patch count rotated, OPCR) of tooth crown surfaces of maxillary postcanine series in living bears. Our main goal is to explore the relationship between these topographic shape descriptors and feeding behaviour. Finally, we use this information as a template to make dietary inferences in the cave bear (*U. spelaeus s.l.*) and to discuss possible extinction causes.

2. Material and methods

We sampled the maxillary tooth rows from P^4 to M^2 of 86 individuals, including a total of 258 teeth, belonging to extant and extinct bear species from different museum collections (see electronic supplementary material, table S1). Our sample includes all known extinct species and subspecies of cave bears (*U. spelaeus s.l.*) [11]: *U. ingressus* and *U. spelaeus* (*U. spelaeus spelaeus*, *U. spelaeus eremus* and *U. spelaeus ladinicus*) [12]. We used a comparative sample data of all living bear species: *A. melanoleuca*, *Helarctos malayanus*, *Melursus ursinus*, *Tremarctos ornatus*, *U. americanus*, *U. maritimus*, *U. thibetanus* and *U. arctos*. Tooth rows with cracked or chipped teeth were discarded, and only fully occluding unworn or lightly worn teeth were considered in the analyses.

High-resolution polyurethane dental replicas of each maxillary series (P^4–M^2) were produced from polyvinylsiloxane-base moulds and scanned using a Roland LPX-600 at 0.2 mm resolution following Figueirido *et al*. (2017) [13] (see electronic supplementary material). Subsequently, we measured a set of 3D-topographic shape metrics from triangulated polygonal mesh data for each tooth row using MorphoTester [9]: (i) DNE [14]; (ii) RFI [15] and (iii) complexity, using OPCR [16,17].

DNE quantifies the amount of bending across a surface, reflecting the relative surface curvature and undulation, irrespective of structure size or orientation [9,14]. Higher DNE values represent sharpened edges and troughs [14]. RFI was calculated as a simple ratio of the 3D crown surface area (3*da*) divided by the two-dimensional (2D) projected surface area (2*da*) [9,15], providing the relative tooth crown height [17,18]. Finally, OPCR was used to quantify complexity with a minimum patch size of five polygons [9]. OPCR was calculated by dividing the occlusal surface into contiguous patches of equal orientation (45° sectors). The number of patches was counted and averaged following eight successive rotations of 5.625° around the z-axis [9].

To explore the association of size with DNE, RFI and OPCR, we regressed these metrics against the 2*da* (mm^2) of each tooth row (P^4–M^2) as a proxy for size (both log-transformed). We also computed phylogenetically independent contrast analyses [19] of DNE, RFI, OPCR and 2*da* using the R package GEIGER [20], and we regressed the contrasts for the three topographic shape metrics on the contrast for 2*da*.

We assembled a phylogenetic tree using Mesquite [21] to explore the phylogenetic patterns of DNE, RFI and OPCR. The relationships of living bears were taken from the previous study [22] based on ancient mitogenomes, and the phylogenetic relationships of cave bears were based on the previous phylogenetic analyses [23].

We calculated Pagel's lambda statistic for continuous traits [24] to assess the phylogenetic signal in DNE, RFI and OPCR, and the phylogenetic variation of the three variables was illustrated by traitgrams [25] using the R package Phytools [26].

To test the association between DNE, RFI, OPCR and feeding behaviour in living bears, we used previously established dietary groupings [7]. The eight species of living bears were classified into three broad dietary categories to facilitate the ecomorphological comparisons: (i) omnivores, feeding less than 50% soft mast; more than 15% hard mast (*U. arctos* and *U. thibetanus*); (ii) folivores-frugivores, feeding more than 50% soft mast and less than 15% hard mast (*U. americanus* and *T. ornatus*) and (iii) faunivores, feeding more than 50% of animal protein, either insects (*H. malayanus* and *M. ursinus*) or vertebrates (*U. maritimus*). The giant panda (*A. melanoleuca*) was assigned to an independent category [7] owing to its highly specialized diet based on bamboo [27]. We assessed the relationship of DNE, RFI, OPCR and feeding behaviour using a phylogenetic ANOVA [28] with GEIGER [20], and assuming Brownian motion. We used 1000 replicates to test for statistical significance. Finally, a principal component analysis (PCA) on the variance–covariance matrix of DNE, RFI and OPCR (converted to *Z*-scores) was performed with PAST 4.02 [29] to calculate the specific patterns from topographic metrics that account for most of the variability observed among dietary groupings.

3. Results

The giant panda (*A. melanoleuca*) showed the highest DNE values, followed by cave bears (figures 1*a*, 2*a*, table 1). The omnivorous bears exhibited intermediate DNE values, followed by the faunivores. The folivores-frugivores reached the lowest DNE values among the sample (figure 1*a*). The same trend among dietary groupings was observed for OPCR (figures 1*c*, 2*c*); however, the RFI value (figure 1*b*) did not distinguish among dietary groupings (figure 2*b*). The results of the phy-ANOVA indicated that both DNE and OPCR are significantly associated with feeding behaviour in living taxa, even when taking phylogeny into account (DNE: $F = 44.509$, $p_{phy} = 0.00693$; OPCR: $F = 44.909$, $p_{phy} = 0.00597$), but this was not the case for RFI ($F = 0.4725$, $p_{phy} = 1.7265$).

The phylogenetic signals of both DNE ($\lambda = 0.973$; $p = 0.01$) and OPCR ($\lambda = 0.985$; $p = 0.02$) were statistically significant, but RFI was statistically independent of phylogeny ($\lambda = 6.6107 \times 10^{-5}$; $p > 0.05$). This pattern was also confirmed by the traitgrams (figure 2*d–f*), as the distribution of both DNE and OPCR preserves a clear phylogenetic structure across species, but RFI distribution does not seem to be influenced by phylogeny [25].

The bivariate regressions of both DNE and OPCR against the surface area (2*da*) of the upper tooth rows (figure 2*g–h*) indicated that variation in both topographic metrics is significantly influenced by tooth size (DNE: $R^2 = 0.632$, $p < 0.001$; OPCR: $R^2 = 0.812$, $p < 0.001$). By contrast, the bivariate regression of RFI against 2*da* was not statistically significant ($R^2 = 0.010$; $p = 0.355$), which indicated that RFI is not influenced by tooth size. The association between the contrasted OPCR and 2*da* ($R^2 = 0.5207$; $F = 10.87$; $p = 0.008$) was statistically significant. However, the association between the contrasted RFI and 2*da* ($R^2 = 0.2216$; $F = 2.847$, $p = 0.122$), as well as DNE and 2*da* ($R^2 = 0.2855$; $F = 3.996$; $p = 0.073$) were not statistically significant.

The morphospace depicted from the PCA performed from topographic metrics (DNE, RFI and OPCR) yielded two significant eigenvectors, which jointly explained 98% of the original variance (figure 2*i*; electronic supplementary

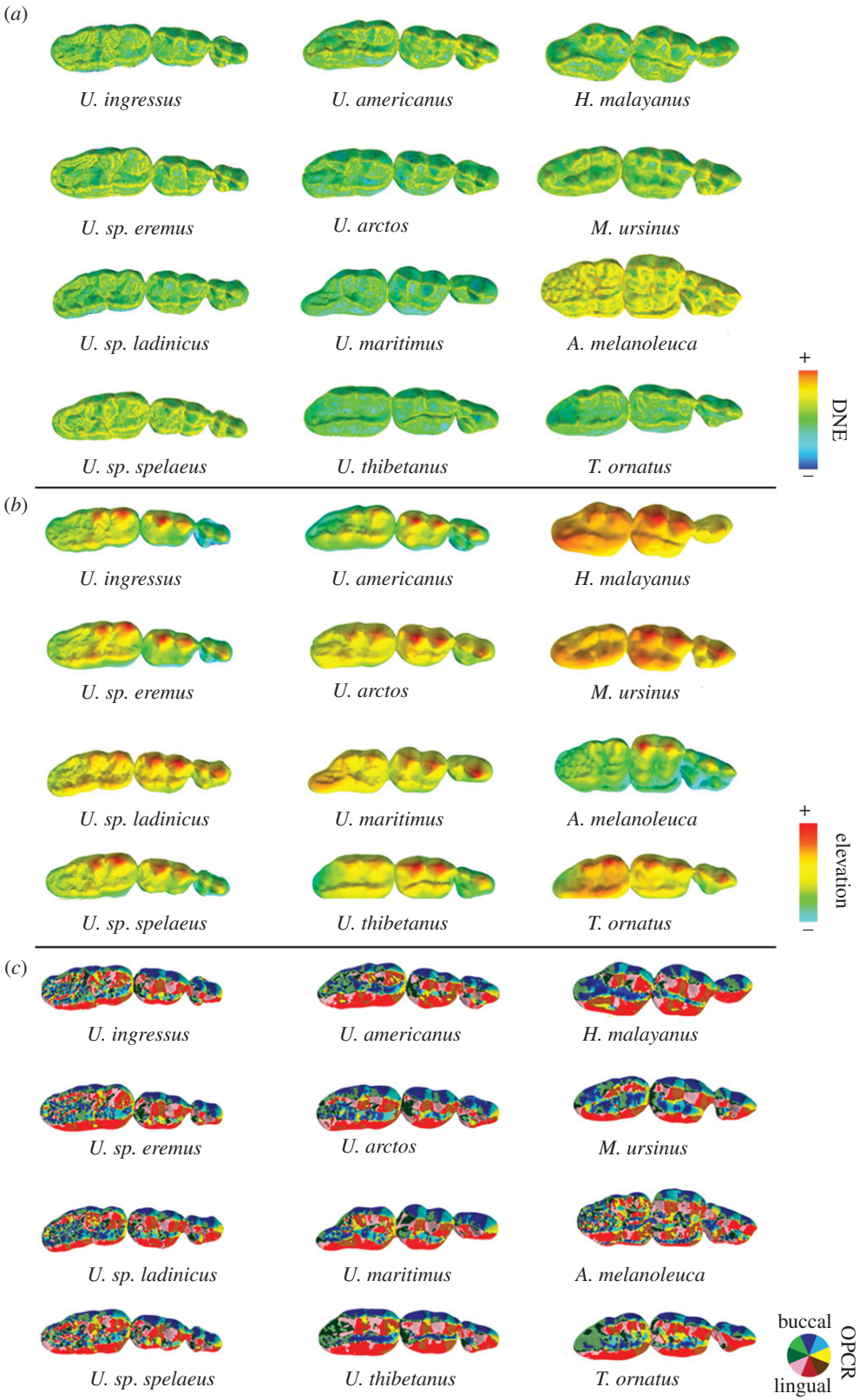

Figure 1. Occlusal views of upper tooth row (P^4–M^2) triangulated meshes displaying morphometric maps for (*a*) Dirichlet normal energy (DNE), (*b*) elevation for surface relief index (RFI) calculation and (*c*) orientation patch count rotated (OPCR) topographic metrics applied with MorphoTester [9]. Only one specimen per species is shown. Warmer (red) and cooler (blue) colours for DNE and elevation maps indicate higher and lower curvature and crown height, respectively. OPCR complexity maps from triangulated meshes indicate surface orientation patches (see colour wheel). Mesial: right.

material, table S2, electronic supplementary material). The factor loadings of the variables on each eigenvector indicated that although both the giant panda and the cave bears were characterized by high values of DNE and OPCR, the faunivores and folivores-frugivores were characterised by low values of both variables. Omnivores were characterized by intermediate values.

4. Discussion

Among living and extinct bears, phylogenetic signal is present on dental topographic curvature and complexity but not on relief, which indicates a clear phylogenetic structure on both curvature and complexity. Moreover, the phylogenetic ANOVA demonstrated that both variables are

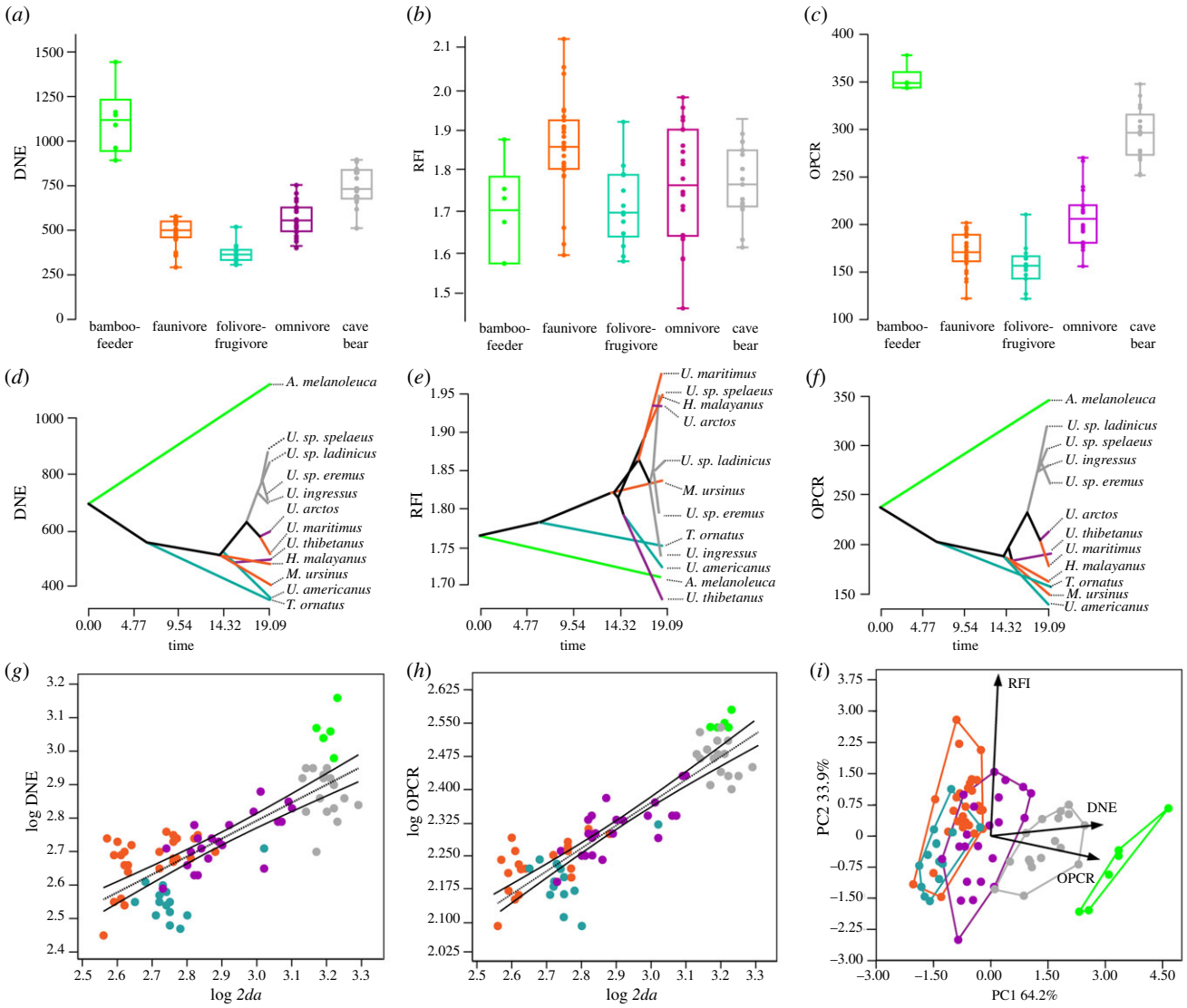

Figure 2. Results of dental topographic analysis. Box-plots for (*a*) DNE, (*b*) RFI and (*c*) OPCR by feeding behaviour in living taxa and cave bears. Boxes enclose 25%–75% percentile values, the horizontal bar indicates the median value and whiskers denote range. Individual values are plotted. Traitgrams for (*d*) DNE, (*e*) RFI and (*f*) OPCR in living taxa and cave bears (the same colour coding as feeding behaviour is used). Bivariate plots for (*g*) DNE and (*h*) OPCR against two-dimensional surface area (2*da*). Dotted lines denote linear regressions; 95% prediction intervals are shown. (*i*) Bivariate plot depicted from the scores on the first two eigenvectors obtained in PCA computed from the three topographic (DNE, RFI and OPCR) metrics. Convex hulls show the distribution limits of each dietary group considered. The labelled rays show the loadings for topographic metrics onto PC1 and PC2 axes. In green, the bamboo-feeder giant panda; in orange, the faunivores; in purple, the omnivores (hard mast specialists); in dark green, the folivore-frugivores (soft mast specialists); and in grey, the cave bears.

significantly associated with feeding behaviour, whereas topographic relief is not.

Dental topographic curvature, relief and complexity are associated with size among species (figure 2*g*,*h*) but, as indicated by the independent contrast analysis, this association does not result from phylogenetic correlation for complexity. Previous authors have demonstrated that cave bears follow a different trend of increasing tooth-root areas across maxillary dental series [7] from any living species; cave bears exhibit a continuous increase from P^4 to M^2 in tooth-root area values, reaching M^2 values similar to those of the giant panda (*A. melanoleuca*). Our results suggest that this trend of increasing tooth-root areas across P^4 to M^2 of cave bears [7] also entails an increase in curvature and complexity in their upper teeth crown surfaces. In general, a larger tooth can process more food with each bite, either through a larger area of contact or through the formation of a longer blade [30–35].

The PCA performed from the shape descriptor metrics revealed an ordination according to feeding behaviour (figure 2*i*). The giant pandas and cave bears show extreme positive scores on PC1 (i.e. high OPCR and DNE values), whereas intermediate scores were observed for the omnivores that specialize in feeding on a hard mast (i.e. fruits and seeds with a hard protective covering, including acorns and pine seeds [36], and roots and tubercles). By contrast, the faunivores and folivores-frugivores exhibited extreme negative scores. This overlap between the folivores-frugivores and the faunivores likely relates to the fact that folivores-frugivores are soft mast specialists (feeding mainly on fleshy fruits or strobili that are softer than hard mast items e.g. [36]). Therefore, based on our findings, topographic metrics are more closely correlated with the mechanical properties of the material than with the type of food ingested.

The PCA also shows evidence that cave bears combine values of curvature and complexity in a unique manner

Table 1. Summary statistics (mean ± 1 s.d.) for DNE, RFI, OPCR and surface area (2*da*) obtained from the upper P^4–M^2 dental series in living and extinct bears.

taxon	*n*	DNE	RFI	OPCR	surface area (2*da*)
A. melanoleuca	6	1121.34 ± 195.8	1.69 ± 0.1	354.15 ± 12.9	1601.62 ± 76.8
H. malayanus	11	481.85 ± 78.7	1.86 ± 0.1	164.45 ± 19.6	440.09 ± 64.2
M. ursinus	5	409.34 ± 56.3	1.72 ± 0.1	172.13 ± 23.7	454.77 ± 68.1
T. ornatus	7	357.60 ± 37.6	1.72 ± 0.1	162.02 ± 10.6	518.87 ± 40.3
U. americanus	7	364.58 ± 69.9	1.70 ± 0.08	152.89 ± 29.6	639.73 ± 181.2
U. arctos	12	597.27 ± 91.8	1.85 ± 0.1	220.97 ± 27.8	972.97 ± 207.2
U. maritimus	11	520.37 ± 40.5	1.88 ± 0.1	186.28 ± 13.6	629.53 ± 63.7
U. thibetanus	10	494.58 ± 65.5	1.67 ± 0.1	192.25 ± 23.3	647.28 ± 62.7
U. sp. *ladinicus*†	4	854.44 ± 48.6	1.80 ± 0.07	328.06 ± 19.5	1537.39 ± 119.8
U. sp. *spelaeus*†	3	816.72 ± 71.1	1.86 ± 0.02	306.43 ± 7.3	1429.08 ± 74.9
U. sp. *eremus*†	4	693.52 ± 90.5	1.74 ± 0.04	279.90 ± 22.02	1587.02 ± 135.6
U. ingressus†	6	699.09 ± 95.8	1.70 ± 0.08	289.88 ± 28.5	1597.43 ± 170.1

among living bears, as evidenced by their position in the empty space of figure 2*i*. We hypothesized that cave bears were feeding on a resource that possessed intermediate mechanical properties to bamboo and hard mast. No living bear currently exploits this feeding resource, most likely because it was only present in the high-alpine biomes that cave bears inhabited. Given that both complexity and curvature are highly influenced by tooth size, we also hypothesize that increasing upper tooth surface areas also increase the values of both topographic variables, and probably, also their chewing efficiency.

In any case, our results indicate that giant pandas show the highest values of curvature and complexity among the sample, which should relate to their peculiar diet, feeding on bamboo [27,37]. Moreover, previous authors [38] have demonstrated that primate species with the most complex teeth are those that consume extremely fibrous vegetation, such as bamboo-eating lemurs. The second group with the highest values of complexity is the cave bears, which may indicate that they were probably feeding on hard materials of low quality, such as highly fibrous vegetal resources.

Although hypothesizing on the specific vegetal resource that cave bears were specialized to feed on is tempting, our results indicate that cave bears were specialized to feed upon tough vegetal resources of the high-alpine biome, which supports the climate-driven hypothesis to explain their extinction at the beginning of the Last Glacial Maximum when the primary productivity that the cave bear fed upon was dramatically lowered [3–5].

Data accessibility. Pérez-Ramos A, Romero A, Rodriguez E, Figueirido B. 2020. Data from: Three-dimensional dental topography and feeding ecology in the extinct cave bear. Dryad Digital Repository (doi:10.5061/dryad.95x69p8j9).

Authors' contribution. B.F. conceived the study; B.F., A.P.-R. and A.R. designed research. A.P.-R., A.R. and E.R. collected data. B.F., A.R. and A.P.-R. analysed data. B.F. wrote the paper with the input of A.R., A.P.-R. and E.R. All authors agree to be held accountable for the content of the manuscript and approve the final version.

Competing interests. We declare we have no competing interests.

Funding. This study has been funded by the Spanish Ministry of Economy and Competitiveness-MEC (CGL2012-37866, CGL2015-68300P) and Junta de Andalucía (UMA18-FEDERJA-188) to B.F.

Acknowledgements. We would like to thank American Museum of Natural History (New York, USA), the Natural Museum of Scotland, the Museum für Naturkunde, the University of Vienna Institution of Palaeontology, and collections of the Valladolid University for allowing us data acquisition. We appreciate the fossil material reviewed by Professor Gernot Rabeder (University of Vienna) and Dr Paco Pastor (University of Valladolid, Spain). The University of Málaga imaging centre scanned the dental moulds and two anonymous reviewers improved the rigour of the manuscript contents.

References

1. Figueirido B, van Heteren AH. 2019 The story continues: recent advances on the life and death of the Pleistocene cave bear. *Hist. Biol.* **31**, 405–409. (doi:10.1080/08912963.2018.1436426)
2. Bocherens H. 2019 Isotopic insights on cave bear palaeodiet. *Hist. Biol.* **31**, 410–421. (doi:10.1080/08912963.2018.1465419)
3. Terlato G, Bocherens H, Romandini M, Nannini N, Hobson KA, Peresani M. 2018 Chronological and isotopic data support a revision for the timing of cave bear extinction in Mediterranean Europe. *Hist. Biol.* **31**, 474–484. (doi:10.1080/08912963.2018.1448395)
4. Stiller M *et al.* 2010 Withering away—25,000 years of genetic decline preceded cave bear extinction. *Mol. Biol. Evol.* **27**, 975–978. (doi:10.1093/molbev/msq083)
5. Mondanaro A *et al.* 2019 Additive effects of climate change and human hunting explain population decline and extinction in cave bears. *Boreas* **48**, 605–615. (doi:10.1111/bor.12380)
6. Pérez-Ramos A, Tseng ZJ, Grandal-D'Anglade A, Rabeder G, Pastor FJ, Figueirido B. 2020 Biomechanical simulations reveal a trade-off between adaptation to glacial climate and dietary niche versatility in European cave bears. *Sci. Adv.* **6**, eaay9462. (doi:10.1126/sciadv.aay9462)
7. Pérez-Ramos A, Kornelius K, Van Heteren AH, Rabeder G, Grandal-D'Anglade A, Pastor FJ, Serrano FJ, Figueirido B. 2019 A three-dimensional analysis of tooth-root morphology in living bears and implications for feeding behaviour in the extinct cave bear. *Hist. Biol.* **31**, 461–473. (doi:10.1080/08912963.2018.1525366)
8. Lucas PW. 2004 *Dental functional morphology: How teeth work*. Cambridge, UK: Cambridge University Press.

9. Winchester JM. 2016 MorphoTester: an open source application for morphological topographic analysis. *PLoS ONE* **11**, e0147649. (doi:10.1371/journal.pone.0147649)
10. Evans AR. 2013 Shape descriptors as ecometrics in dental ecology. *Hystrix* **24**, 133–140. (doi:10.4404/hystrix-24.1-6363)
11. Baca M, Popović D, Stefaniak K, Marciszak A, Urbanowski M, Nadachowski A, Mackiewicz P. 2016 Retreat and extinction of the Late Pleistocene cave bear (Ursus spelaeus sensu lato). *Sci. Nat.* **103**, 11–12. (doi:10.1007/s00114-016-1414-8)
12. Knapp M. 2019 From a molecules' perspective – contributions of ancient DNA research to understanding cave bear biology. *Hist. Biol.* **31**, 442–447. (doi:10.1080/08912963.2018.1434168)
13. Figueirido B, Pérez-Ramos A, Schubert BW, Serrano F, Farrell AB, Pastor FJ, Neves Aline A, Romero A. 2017 Dental caries in the fossil record: a window to the evolution of dietary plasticity in an extinct bear. *Sci. Rep.* **7**, 1–7. (doi:10.1038/s41598-017-18116-0)
14. Bunn JM, Boyer DM, Lipman Y, St Clair EM, Jernvall J, Daubechies I. 2011 Comparing Dirichlet normal surface energy of tooth crowns, a new technique of molar shape quantification for dietary inference, with previous methods in isolation and in combination. *Am. J. Phys. Anthropol.* **145**, 247–261. (doi:10.1002/ajpa.21489)
15. Boyer DM. 2008 Relief index of second mandibular molars is a correlate of diet among prosimian primates and other euarchontan mammals. *J. Hum. Evol.* **55**, 1118–1137. (doi:10.1016/j.jhevol.2008.08.002)
16. Evans AR, Wilson GP, Fortelius M, Jernvall J. 2007 High-level similarity of dentitions in carnivorans and rodents. *Nature* **445**, 78–81. (doi:10.1038/nature05433)
17. Pineda-Munoz S, Lazagabaster IA, Alroy J, Evans AR. 2017 Inferring diet from dental morphology in terrestrial mammals. *Meth. Ecol. Evol.* **8**, 481–491. (doi:10.1111/2041-210X.12691)
18. Berthaume MA, Winchester J, Kupczik K. 2019 Effects of cropping, smoothing, triangle count, and mesh resolution on dental topographic metrics. *PLoS ONE* **14**, e0216229. (doi:10.1371/journal.pone.0216229)
19. Felsenstein J. 1985 Phylogenies and the comparative method. *Am. Nat.* **125**, 1–15. (doi:10.1086/284325)
20. Harmon LJ, Weir JT, Brock CD, Glor RE, Challenger W. 2008 GEIGER: investigating evolutionary radiations. *Bioinformatics* **24**, 129–131. (doi:10.1093/bioinformatics/btm538)
21. Maddison WP, Maddison DR. 2018 Mesquite: a modular system for evolutionary analysis. Version 3.51. See http://www.mesquiteproject.org.
22. Krause J *et al.* 2008 Mitochondrial genomes reveal an explosive radiation of extinct and extant bears near the Miocene-Pliocene boundary. *BMC Evol. Biol.* **8**, e220. (doi:10.1186/1471-2148-8-220)
23. Stiller M, Molak M, Prost S, Rabeder G, Baryshnikov G, Rosendahl W, Germonpré M. 2014 Mitochondrial DNA diversity and evolution of the Pleistocene cave bear complex. *Quatern. Int.* **339**, 224–231. (doi:10.1016/j.quaint.2013.09.023)
24. Blomberg SP, Garland TJr, Ives AR. 2003 Testing for phylogenetic signal in comparative data: behavioral traits are more labile. *Evolution* **57**, 717–745. (doi:0.1111/j.0014-3820.2003.tb00285.x)
25. Münkemüller T, Lavergne S, Bzeznik B, Dray S, Jombart T, Schiffers K, Thuiller W. 2012 How to measure and test phylogenetic signal. *Methods Eco. Evol.* **3**, 743–756. (doi:10.1111/j.2041-210X.2012.00196.x)
26. Revell LJ. 2012 Phytools: an R package for phylogenetic comparative biology (and other things). *Methods Ecol. Evol.* **3**, 217–223. (doi:10.1111/j.2041-210X.2011.00169.x)
27. Figueirido B, Tseng ZJ, Martín-Serra A. 2013 Skull shape evolution in durophagous carnivorans. *Evolution* **67**, 1975–1993. (doi:10.1111/evo.12059)
28. Garland T Jr, Dickerman AW, Janis CM, Jones JA. 1993 Phylogenetic analysis of covariance by computer simulation. *Syst. Biol.* **42**, 265–292. (doi:10.1093/sysbio/42.3.265)
29. Hammer Ø, Harper DA, Ryan PD. 2001 PAST: Paleontological statistics software package for education and data analysis. *Palaeontol. Electron.* **4**, 9.
30. Evans AR, Pineda-Munoz S. 2018 Inferring mammal dietary ecology from dental morphology. In *Methods in paleoecology* (eds D Croft, D Su, S Simpson), pp. 37–51. Cham, Switzerland: Springer.
31. Vizcaíno SF, Bargo MS, Cassini GH. 2006 Dental occlusal surface area in relation to food habits and other biologic features in fossil Xenarthrans. *Ameghiniana* **43**, 11–26.
32. Janis CM. 1990 Correlation of cranial and dental variables with dietary preferences in mammals: a comparison of macropodoids and ungulates. *Mem. Queensl. Mus.* **28**, 349–366.
33. Janis CM. 1995 Correlations between craniodental morphology and feeding behavior in ungulates: reciprocal illumination between living and fossil taxa. In *Functional morphology in vertebrate paleontology* (ed JJ Thomason), pp. 78–98. Cambridge, NJ: Cambridge University Press.
34. Janis CM, Constable E. 1993 Can ungulate craniodental features determine digestive physiology? *J. Vert. Paleontol.* **13**, 43A.
35. Mendoza M, Janis CM, Palmqvist P. 2002 Characterizing complex craniodental patterns related to feeding behaviour in ungulates: a multivariate approach. *J. Zool.* **258**, 223–246. (doi:10.1017/S0952836902001346)
36. Janis CM, Fortelius M. 1988 On the means whereby mammals achieve increased functional durability of their dentitions, with special references to limiting factors. *Biol. Rev.* **63**, 197–230. (doi:10.1111/j.1469-185X.1988.tb00630.x)
37. Mattson DJ. 1998 Diet and morphology of extant and recently extinct northern bears. *Ursus* **10**, 479–496.
38. Eronen JT, Zohdy S, Evans AR, Tecot SR, Wright PC, Jernvall J. 2017 Feeding ecology and morphology make a bamboo specialist vulnerable to climate change. *Curr. Biol.* **27**, 3384–3389. (doi:10.1016/j.cub.2017.09.050